An application for nonlinear control by input-output linearization technique for pm synchronous motor drive for electric vehicles

Boucha Abdellah[1], Hazzab Abdeldjebar[1], Khessam Medjdoub[2]
[1]Laboratory of Command, Analysis and Optimization of Electro-Energetic Systems (CAOSEE), Tahri Mohamed University, Bechar, Algeria
[2]Institute of Science and Technology, University Center Salhi Ahmed, Naama, Algeria

Article Info	ABSTRACT
Article history: Received Jan 17, 2022 Revised Jul 3, 2022 Accepted Jul 18, 2022 *Keywords:* Electric vehicle Input-output feedback Linearization Nonlinear control PMSM Sliding mode control Traction control	This paper leads to present the modified approach of the speed control for permanent magnet synchronous motors applied to electric vehicles using a nonlinear control. The motor's nonlinear dynamics are transformed into a linearized system model using the input-output feedback linearization technique. There are two permanent magnet synchronous motors (PMSM) in the propulsion model. In order to improve the motor's output torque, the direct component of the current is adjusted to zero. The electronic differential, which is used in the calculations, enables each driving wheel to be controlled individually at each curve. The MATLAB/Simulink software is used to implement modeling and simulation in order to assess the effectiveness of the suggested solution. Simulation studies are used to confirm the efficacy of the proposed technique. The obtained results signify that this approach is more accurate. *This is an open access article under the <u>CC BY-SA</u> license.*

Corresponding Author:

Boucha Abdellah
Laboratory of Command, Analysis and Optimization of Electro-Energetic systems (CAOSEE)
Tahri Mohamed University, Béchar, Algeria
Email: boucha_a@yahoo.fr

1. INTRODUCTION

With its high performance, permanent magnet synchronous motors (PMSM) has been hardlyexploited inquite high-performance drives such as machinetools and industrial robots. The fundamental drawback of PMSM, however, is the requirement for a complicated control unit that, because of its extremely non-linear properties, guarantees high-efficiency electric drive applications. The development of permanent magnet technology has led to the widespread use PMSM for various engineering applications, especially in variable-speed motors and electric vehicles were presented in [1], [2]. An efficient technique for controlling nonlinear systems is to linearize input- output feedback.

This section describes the nonlinear control strategy that was simply input output feedback control and depends on differential geometry techniques. The motor model can be split using these techniques into two separate monovariable linear subsystems. A perfect arrangement of the poles that reveals the dynamics of each subsystem was presented by Rebouh *et al.* [3].

The speed parameters of this controller are used within a drive system managessential objectives to reunite with other important criteria of the high-performance drive. Based on the literature, nonlinear systems have been traditionally developed by using classical linear control methods. These methods are only operational for a small operating range. In the case of a huge required operating range, the linear controller is

no longer able to perform poorly. However, nonlinear controllers may operate the nonlinearities in range operations directly [4], [5].

Without a speed sensor, the research [6] described a direct torque control/sliding mode control DTC/SMC for IM training. The control method for an induction motor IM drive is built on the combination of SMC and stator flux field orientation control as presented in [6]. As an input-output feedback linearization technique, the vector control scheme's internal dynamics cannot be analytically shown to be stable under transient and steady state conditions. This means that unless the controller gains are properly set with more precision, the control system is only locally stable. In order to drive an induction motor without a sensor, The feedforward control principle, DTC, and modulation of spatial vectors (SVM) approach have been integrated and utilized in [7]. Because robust induction, a sort of field-oriented control, allows for extremely precise machine control, its development [8]–[15] marked a significant turning point in the field of electric drives.

The following describes how the paper is structured: The PMSM mathematical model is described in the second section. The third portion covers the whole design of control utilizing input-output linearization theory. Section 4 describes the parts of the electric traction system, whereas section 5 describes the parts of the electric differential system. Section 4 contains the simulation's results as well as a discussion of them. The last part explains the results obtained using the proposed controller.

2. PMSM MATHEMATICAL MODEL

According to the design in [12]-[18], PMSM drives the electric car's two rear wheels. More details based on the mathematical formulations can be found in the following section.

2.1. Description of machine equations

In this section, the mathematical representation of the PMSM in the rotor frame (d-q) can be written as assuming that the PMSM is three-phase with balanced windings and no saturation [12].

$$\begin{pmatrix} v_d \\ v_q \end{pmatrix} = \begin{bmatrix} R_s + pL_d & -w_r^* L_q \\ w_r^* L_d & R_s + pL_q \end{bmatrix} \begin{pmatrix} i_d \\ i_q \end{pmatrix} + \begin{pmatrix} 0 \\ w_r^* \varphi_f \end{pmatrix} \tag{1}$$

Applying the transformation of (1) from the d-q coordinate to α-β coordinate, is given by (2) and (3).

$$\begin{cases} v_\alpha = R_s i_\alpha + w_r(L_d - L_q)i_\beta + E_\alpha \\ v_\beta = R_s i_\beta + L_d p i_\beta - w_r(L_d - L_q)i_\alpha + E_\beta \end{cases} \tag{2}$$

$$\begin{cases} E_\alpha = \{((L_d - L_q)(w_r p i_d - p i_q) + w_r \varphi_f\}(-sin\theta_r) \\ E_\beta = \{(L_d - L_q)(w_r p i_d - p i_q) + w_r \varphi_r\}(cos\theta_r) \end{cases} \tag{3}$$

Where: (v_α, v_β and i$_\alpha$, i_β) are (α, β) axis voltage/current components, θ_r is Rotor angular.

Based on in (2), In the following formula, the mathematical models for PMSM with fixed frames of reference (α, β) are presented by (4).

$$\begin{pmatrix} \frac{di_\alpha}{dt} \\ \frac{di_\beta}{dt} \end{pmatrix} = \begin{pmatrix} -\frac{R_s}{L_d} & -w_r\left(\frac{L_d - L_q}{L_d}\right) \\ w_r\left(\frac{L_d - L_q}{L_d}\right) & -\frac{R_s}{L_d} \end{pmatrix} \begin{pmatrix} i_\alpha \\ i_\beta \end{pmatrix} + \begin{pmatrix} -\frac{1}{L_d} & 0 \\ 0 & \frac{1}{L_d} \end{pmatrix} \begin{pmatrix} E_\alpha \\ E_\beta \end{pmatrix} + \frac{1}{L_d}\begin{pmatrix} v_\alpha \\ v_\beta \end{pmatrix} \tag{4}$$

The stator flux linkage and current expression for the electromagnetic torque (T_e) of the PMSM as in (5).

$$T_e = \frac{3}{2} p (\varphi_\alpha i_\beta - \varphi_\beta i_\alpha) \tag{5}$$

The following formulation represents the state flux linkage in the α-β by (6).

$$\begin{cases} \frac{d\varphi_\alpha}{dt} = v_\alpha - R_s i_\alpha \\ \frac{d\varphi_\beta}{dt} = v_\beta - R_s i_\beta \end{cases} \tag{6}$$

The stator flux linkage's amplitude (φ_s) as in (7).

$$\varphi_s = \sqrt{\varphi_\alpha^2 + \varphi_\beta^2} \tag{7}$$

The dynamic equation is delivered by (8).

$$j\frac{dw_r}{dt} = p(T_e - T_L) - fw_r \tag{8}$$

A dynamic model of the PM synchronous motors can be expressed using (2)-(8) as in (9).

$$\begin{cases} \begin{pmatrix} \frac{di_\alpha}{dt} \\ \frac{di_\beta}{dt} \end{pmatrix} = \begin{pmatrix} -\frac{R_s}{L_d} & 0 \\ 0 & -\frac{R_s}{L_d} \end{pmatrix}\begin{pmatrix} i_\alpha \\ i_\beta \end{pmatrix} + \\ \begin{pmatrix} -\frac{1}{L_d} & 0 \\ 0 & -\frac{1}{L_d} \end{pmatrix}\begin{pmatrix} E_\alpha \\ E_\beta \end{pmatrix} + \frac{1}{L_d}\begin{pmatrix} v_\alpha \\ v_\beta \end{pmatrix} \\ T_e = \frac{3}{2}p\varphi_f(i_\beta cos\theta_r - i_\alpha sin\theta_r) \\ \frac{dw_r}{dt} = \frac{p}{j}(T_e - T_L) - \frac{f}{j}w_r \end{cases} \tag{9}$$

3. ELECTRIC DRIVE SYSTEM COMPONENT MODELING

In this section, electric drive system component modeling is presented. Figure 1 depicts a general representation of an electric traction system that combined battery, inverter, PMSM, gears, and wheel. However, the PMSM speed controlled by electrical differential. This structure applied for two back wheels.
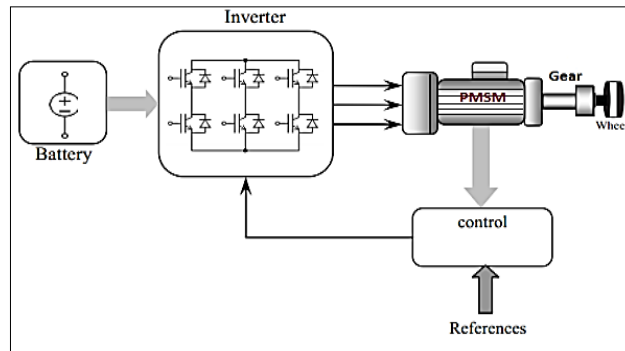

Figure 1. The electric drive system's chain

3.1. Description of energy source

In this section, a description of the energy source is provided. A lithium-ion battery system serves as the typical power source. Compared to other types of rechargeable batteries, lithium-ion battery innovation has benefits in the main aim of specific energy, specific power, and service life.

3.2. Model with inverters

In this example, the current battery in the electric traction system is provided to generate three balanced phases of variable frequency alternating current in [19].

$$\begin{bmatrix} v_a \\ v_b \\ v_c \end{bmatrix} = \frac{U_{dc}}{3}\begin{pmatrix} 2 & -1 & -1 \\ -1 & 2 & -1 \\ -1 & -1 & 2 \end{pmatrix}\begin{bmatrix} S_a \\ S_b \\ S_c \end{bmatrix} \tag{10}$$

3.3. Analysis of vehicle dynamics

The road load F_{res} the formula is based on the principles of vehicle dynamics and aerodynamics [5]–[10].

$$F_{rec} = F_{R_r} + F_{S_r} + F_{A_d} \tag{11}$$

F_{R_r}: rolling resistance, F_{S_r} : slope resistance, F_{A_d}:the aerodynamic drag.

$$F_{R_r} = \mu M g \tag{12}$$

$$F_{S_r} = Mg\sin(\alpha) \tag{13}$$

$$F_{A_d} = \frac{1}{2}\rho C_x A_f (v - v_0)^2 \tag{14}$$

4.   EVALUATION OF THE ELECTRIC DIFFERENTIAL AND ITS CONSEQUENCES

Since the two rear wheels are directly driven by two independent motors, the speed of the outer wheel must differ from the speed of the inner wheel when cornering. This need can be easily satisfied if the position encoder can detect the angular position of the steering wheel. More details can be found in Figure 2. Figure 3. Presents the electric differential under the block diagram as applied for the numerical simulations based on the prior equation.
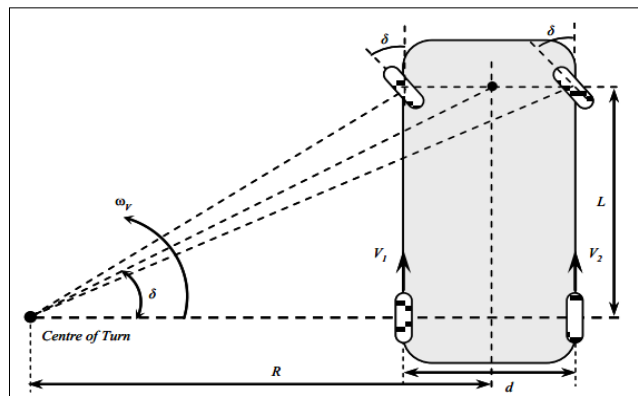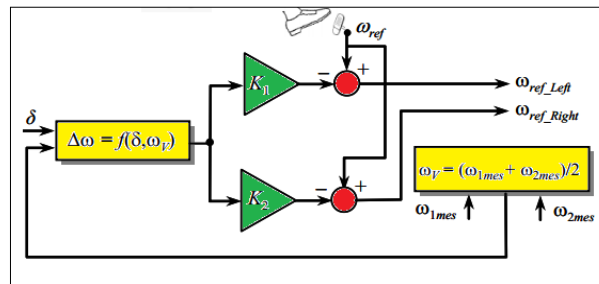

Figure 2. Driving trajectory model

Figure 3. Electronic differential diagram

The driver sets the reference speed when turning the car; if the car goes left, the speed of the right wheel increases and the speed of the left wheel lowers. The following equation expresses the difference in the angular velocities of the driving wheels.

$$\Delta w = w_{mes1} - w_{mes2} = -\frac{d_w \tan\delta}{L_w} w_v \tag{15}$$

Next, the steering angle indicates the direction of the trajectory.

$$\begin{cases} \delta > 0 \rightarrow turn\ldots left \\ \delta < 0 \rightarrow turn\ldots right \\ \delta = 0\ straight\ldots ahead \end{cases} \tag{16}$$

An application for nonlinear control by input-output linearization technique … (Boucha Abdellah)

5. CONTROL OF THE PMSM'S INPUT-OUTPUT LINEARIZATION

The input-output linearization technique converts the nonlinear system into a decoupled linear system by a nonlinear change in coordinates and feedback. The model of the engine in the *d-q* frame of reference is provided [20]–[25], along with simplifying assumptions for the PMSM.

$$
\begin{cases}
\frac{di_d}{dt} = -\frac{R_s}{L_d}i_d + \frac{L_q}{L_d}pw_r i_q + \frac{1}{L_d}u_d \\
\frac{di_q}{dt} = -\frac{R_s}{L_q}i_q + \frac{L_q}{L_d}pw_r i_d - \frac{\varphi_f}{L_q}pw_r + \frac{1}{L_q}u_q \\
\frac{dw_r}{dt} = \frac{3p}{2J}\left(\varphi_f i_q + \lambda i_d i_q\right) - \frac{1}{J}T_L - \frac{B}{J}w_r
\end{cases}
\tag{17}
$$

The T_L is taken out of the equations in this model and will be treated as a disturbance. The dynamics of the system can then be rearranged as seen in (1), (5), and (17).

$$
\dot{x} = f(x) + g_1(x).u_d + g_2(x).u_q
\tag{18}
$$

Where,

$$
\begin{aligned}
x &= \left[i_d i_q w_r\right]^T \\
g_1 &= \left[\frac{1}{L_d} 0 0\right]^T \\
g_2 &= \left[0 \frac{1}{L_d} 0\right]^T
\end{aligned}
\tag{19}
$$

Next, comparing (17) and (18), we can obtain:

$$
f(x) = \begin{bmatrix} f_1 \\ f_2 \\ f_3 \end{bmatrix} = \begin{bmatrix} -\frac{R_s}{L_d}i_d + \frac{L_q}{L_d}pw_r i_q \\ -\frac{R_s}{L_q}i_q + \frac{L_q}{L_d}pw_r i_d - \frac{\varphi_f}{L_q}pw_r \\ \frac{3p}{2J}\left(\varphi_f i_q + \lambda i_d i_q\right) - \frac{B}{J}w_r \end{bmatrix}
\tag{20}
$$

If a direct relation must be established between the outputs *y* and the inputs *u* of the system, the output variable is chosen by $y_1 = i_d$ and $y_2 = w_r$. Consequently, the following could be a simple way to express the output dynamics:

$$
y_1 = i_d = h_1(x), \nabla h_1 = [1\ 0\ 0]
\tag{21}
$$

$$
y_2 = w_r = h_2(x), \nabla h_2 = [0\ 0\ 1]
\tag{22}
$$

The order of the system's relative degree can be used to determine if a nonlinear system admits input-output linearization under the condition of linearization. We determine the output relative degree in order to derive the nonlinear control law. The relative degree of the d-axis current $i_d = y_1$ [21].

$$
\begin{aligned}
\dot{y}_1 &= L_f h_1(x) + L_{g1}h_1(x)u_d + L_{g2}h_1(x)u_q \\
&= -\frac{R_s}{L_d}i_d + \frac{L_q}{L_d}pw_r i_q
\end{aligned}
\tag{23}
$$

$r_1 = 1$ is the relative degree of $y_1(x)$. The diagram of linearized system is presented in Figure 4 with more details.

The mechanical speed's proportional degree is $w_m = y_2$

$$
\begin{aligned}
\dot{y}_2 &= L_f h_2(x) + L_{g1}2(x)u_d + L_{g2}h_1(x)u_q \\
&= \frac{3p}{2J}\left(\varphi_f i_q + \lambda i_d i_q\right) - \frac{B}{J}w_r
\end{aligned}
\tag{24}
$$

We note that the inputs *u* doesn't be shown in (24), a second derivative became then necessary:

$$\ddot{y}_2 = L_f{}^2 h_2(x) + L_{g1}(L_f h_2(x)) u_d + L_{g2}(L_f h_2(x) u_q$$

$$= A\lambda i_q f_1(x) + A(\varphi_f + \lambda i_d) f_2(x) - \frac{B}{J} f_3(x) + \frac{A\lambda}{L_d} i_q u_d + \frac{A(\varphi_f + \lambda i_d)}{L_q} u_q \tag{25}$$

where

$$\Lambda = \frac{3p}{2J} \tag{26}$$

$y_2(x)$ has a relative degree of $r_2 = 2$. The system's relative degree is equal to its order n (which is set to 3). It is a perfectly linear system. By using the (22) and (25):

$$[\dot{y}_1 \ddot{y}_2]^T = \xi(x) + D(x). u \tag{27}$$

where

$$\xi = \left[L_f h_1(x) L_f{}^2 h_2(x)\right]^T$$
$$= \begin{bmatrix} -\frac{R_s}{L_d} i_d + \frac{L_q}{L_d} pw_r i_q \\ A\lambda i_q f_1(x) + A(\varphi_f + \lambda i_d) f_2(x) - \frac{B}{J} f_3(x) \end{bmatrix} \tag{28}$$

and

$$D(x) = \begin{bmatrix} \frac{1}{L_d} & 0 \\ \frac{A\lambda}{L_d} i_q & \frac{A(\varphi_f + \lambda i_d)}{L_q} \end{bmatrix} \tag{29}$$

The output dynamics are of order two even though the system dynamics are of third order, indicating the presence of internal dynamics and the resulting stability, which could be easily verified. With the assumption of $v_1 = \dot{y}_1$ and $v_2 = \ddot{y}_2$ as new state variables in [22]–[27]. We use the following nonlinear state feedback to linearize the motor's input-output behaviours in the closed loop.

$$\begin{bmatrix} u_d \\ u_q \end{bmatrix} = D^{-1}(x) \left(\begin{bmatrix} v_1 \\ v_2 \end{bmatrix} - \xi(x) \right) \tag{30}$$

The decoupling matrix must $D^{-1}(x)$ be invertible. When the linearizing law (30) is applied to the system (27), two mono-variable, linear, and decoupled sub-systems can be created.

$$[\dot{y}_1 \ddot{y}_2]^T = [v_1 v_2]^T \tag{31}$$

The internal inputs (v_1, v_2) are calculated (poles placement) by imposing static modes (i_{dref} and w_{ref}) and an error dynamic.

$$\begin{cases} \dot{e}_{id} + K_d e_1 = 0 \\ \ddot{e}_w + K_{w1} \dot{e}_w + K_{w2} e_w = 0 \end{cases} \tag{32}$$
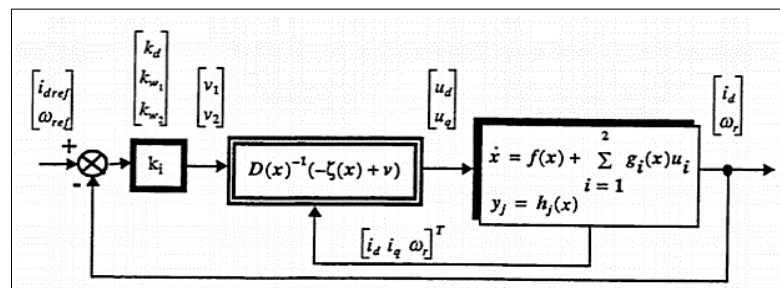

Figure 4. Block diagram of linearized system

6.   RESULTS AND DESCRIPTION

Simulations were run utilizing the model of the drive wheel system to characterize the behavior as presented in Figure 5. They display motor current as well as each motor's speed fluctuation. More details about simulation including discussion ban be found in the following sections.

6.1. In the case of a straight road

During this time, the EV drives at a speed of 80 km/h. Figure 5, provides that the speed of an EV has two phases. In the first phase, a speed of 80 km/h, and between [0 3] sand between [3 5] s in the second phase with a speed equal to 60 km/h. The two back wheels are moving at the same speed, as can be seen. This indicates that in this instance, the electrical differential is inoperative. The following graph indicates that the main change experienced when utilizing F_{pente}= 5.81 between [2 3] s. The torque of the produced motor is audible. The electromagnetic motor torque is significantly improved by the slope effect on both the left and right sides of each motor. Figure 5 serves as an example of the system's behavior.
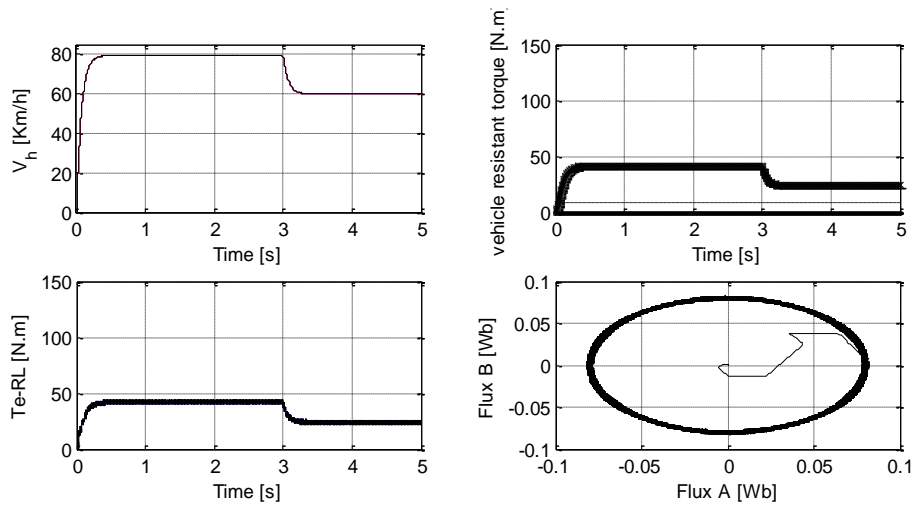

Figure 5. Straight road application

6.2. A 60 km/h curved road is on the right

In this stage, we inform the user that the EV is driving at a speed of 80 km/h. Figure 6 describes the EV speed that has two phases. In the first phase, is located between [0 2] s at 80 km/h and [2 5] s at 60 Km/h. Once this speed is regular, the resistive torque given to the motor wheels as a whole cause the torque to revert to its initial value. Next, in [3.5 4.5] s means the speed changed during the curved road to stabilize the EV.
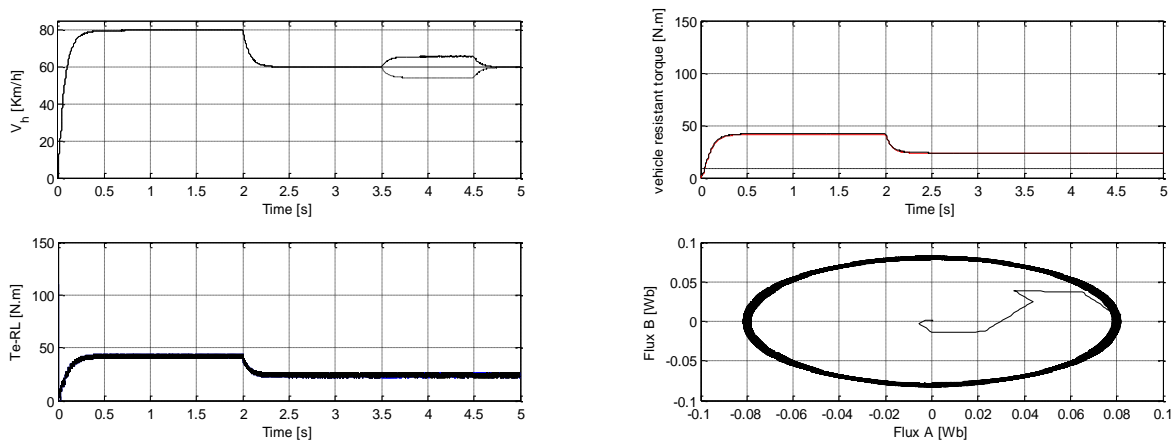

Figure 6. Curved road

7.   CONCLUSION

In the propulsion model, there are two permanent magnet synchronous motors (PMSM). The direct component of the current is set to zero to increase the motor's output torque. Each driving wheel may be separately controlled at each curve according to the electronic differential, which is used in the calculations. The program Matlab/Simulink is used to implement modeling and simulation in order to evaluate the efficacy of the proposed solution. Simulation studies are conducted to verify the effectiveness of the suggested method. The outcomes show that this strategy is more accurate. In future work, a novel application will be provided using different recent techniques and real applications.

REFERENCES

[1]   V. Oghafy, H. Nikkhajoei and J. S. Zamani, "An adaptive controller for sensorless PM synchronous motor drive for electric vehicles," *IEEE Vehicle Power and Propulsion Conference*, 2009, pp. 265-269, doi: 10.1109/VPPC.2009.5289843.

[2]   M Habbab, A Hazzab, and A Alalei, "Real time implementation of nonlinear PI controller for the induction machine control," *Journal of Fundamental and Applied Sciences*, vol. 11, no. 2, pp. 1033-1044, 2019, doi: 10.4314/jfas.v11i2.31.

[3]   S. Rebouh, A. Kaddouri, R. Abdessemed and A. Haddoun, "Nonlinear Control by Input-Output Linearization Scheme for EV Prmanent Magnet Synchronous Motor," *IEEE Vehicle Power and Propulsion Conference*, 2007, pp. 185-190, doi: 10.1109/VPPC.2007.4544122.

[4]   C. K. Lin, T. H. Liu and S. H. Yang, "Nonlinear position controller design with input–output linearization technique for an interior permanent magnet synchronous motor control system," *IET Power Electronics*, vol. 1, no. 1, pp. 14-26, 2008, doi: 10.1049/iet-pel:20070177.

[5]   K. H. Kim and M. J. Youn, "A nonlinear speed control for a PM synchronous motor using a simple disturbance estimation technique," *IEEE Transactions on Industrial Electronics*, vol. 49, no. 3, pp. 524-535, 2002, doi: 10.1109/TIE.2002.1005377.

[6]   C. Lascu, I. Boldea and F. Blaabjerg, "Direct torque control of sensorless induction motor drives: a sliding-mode approach," *IEEE Transactions on Industry Applications*, vol. 40, no. 2, pp. 582-590, 2004, doi: 10.1109/TIA.2004.824441.

[7]   G. A. A. Markadeh and J. Soltani, "Robust Direct Torque Control of An Adjustable Speed Sensorless Induction Machine Drive Using A PI Predictive Controller," *ICPE (ISPE) 논문집*, 2004, pp. 160-164.

[8]   M. E. A. Abdelkoui, and A Hazzab, "Predictive torque control of electric vehicle," *International Journal of Electrical & Computer Engineering,* vol. 9, no. 5, pp. 3522-3530, 2019, doi: 10.11591/ijece.v9i5.pp3522-3530.

[9]   R. Marino, S. Peresada and P. Valigi, "Adaptive input-output linearizing control of induction motors," *IEEE Transactions on Automatic Control*, vol. 38, no. 2, pp. 208-221, 1993, doi: 10.1109/9.250510.

[10]   M. Khessam, A. Hazzab, B. Bouchiba, and M Bendjima, "Fuzzy Adaptive PI Controller for DTFC in Electric Vehicle," *International Journal of Power Electronics and Drive Systems*, vol. 4, no. 4, pp. 557-566, 2014, doi: 10.11591/ijpeds.v4i4.6372.

[11]   A. Haddoun, M. Benbouzid, D. Diallo, R. Abdessemed, J. Ghouili and K. Srairi, "Sliding mode control of EV electric differential system," *ICEM'06*, pp. 6, 2006.

[12]   M. A. Rahman and R. Qin, "A permanent magnet hysteresis hybrid synchronous motor for electric vehicles," in *IEEE Transactions on Industrial Electronics*, vol. 44, no. 1, pp. 46-53, 1997, doi: 10.1109/41.557498.

[13]   M. A. Rahman, D. M. Vilathgamuwa, M. N. Uddin and King-Jet Tseng, "Nonlinear control of interior permanent-magnet synchonous motor," *IEEE Transactions on Industry Applications*, vol. 39, no. 2, pp. 408-416, 2003, doi: 10.1109/TIA.2003.808932.

[14]   A. Laguidi, A. Hazzab, O. Boughazi, and A. Alalei, "Nonlinear PI controller for the control of electric vehicle with two-motor wheel drive," *Journal of Fundamental and Applied Sciences*, vol. 12, pp. 181-197, 2020, doi: 10.4314/JFAS.V12I1.13.

[15]   A. J. Abianeh, "Direct torque and flux control of IPM synchronous motor drive using input-output feedback linearization approach," *IECON 2011 - 37th Annual Conference of the IEEE Industrial Electronics Society*, 2011, pp. 1813-1818, doi: 10.1109/IECON.2011.6119581.

[16]   A. Accetta, M. Cirrincione, F. D'Ippolito, M. Pucci and A. Sferlazza, "Input-Output Feedback Linearization Control with On-Line Inductances Estimation of Synchronous Reluctance Motors," *IEEE Energy Conversion Congress and Exposition (ECCE)*, 2021, pp. 4973-4978, doi: 10.1109/ECCE47101.2021.9595860.

[17]   T. Vajsz, L. Szamel and G. Racz, "A Novel Modified DTC-SVM Method with Better Overload-capability for Permanent Magnet Synchronous Motor Servo Drives," *Periodical Polytechnical Electrical Engineering and Computer Science*, vol. 61, no. 3, pp. 253-263, 2017, doi: 10.3311/PPee.10428.

[18]   Y. Duan and D. M. Ionel, "A Review of Recent Developments in Electrical Machine Design Optimization Methods with a Permanent-Magnet Synchronous Motor Benchmark Study," *IEEE Transactions on Industry Applications*, vol. 49, no. 3, pp. 1268-1275, 2013, doi: 10.1109/TIA.2013.2252597.

[19]   Y. M. Alsayed, A. Maamoun and A. Shaltout, "High Performance Control of PMSM Drive System Implementation Based on DSP Real-Time Controller," *International Conference on Innovative Trends in Computer Engineering (ITCE)*, 2019, pp. 225-230, doi: 10.1109/ITCE.2019.8646462.

[20]   H. H. Hoai, S. C. Chen and C. F. Chang, "Realization of the Neural Fuzzy Controller for the Sensorless PMSM Drive Control System," *Electronics*, vol. 9, no. 9, pp. 1-28, 2020, doi: 10.3390/electronics9091371.

[21]   G. Park, G. Kim and B. G. Gu, "Sensorless PMSM Drive Inductance Estimation Based on a Data-Driven Approach," *Electronics*, vol. 10, no. 7, pp. 1-19, 2021, doi: 10.3390/electronics10070791.

[22]   D. S. Putra, S. C. Chen, H. H. Khong and F. Cheng, "Design and Implementation of a Machine Learning Observer for Sensorless PMSM Drive Control," *Applied Sciences*, vol. 12, no. 6, pp. 1-20, doi: 10.3390/app12062963.

[23]   M. Mehrasa, M. Babaie, M. Sharifzadeh and K. Al-Haddad, "An Input–Output Feedback Linearization Control Method Synthesized by Artificial Neural Network for Grid-Tied Packed E-Cell Inverter," *IEEE Transactions on Industry Applications*, vol. 57, no. 3, pp. 3131-3142, 2021, doi: 10.1109/TIA.2021.3049456.

[24]   W. Gu, X. Zu, L. Quan and Y. Du, "Design and Optimization of Permanent Magnet Brushless Machines for Electric Vehicle Applications," *Energies*, vol. 8, no. 2, pp. 1-13, 2015, doi: 10.3390/en81212410.

[25]   Y. Zafari, A. H. Mazinah and S. S. Majidabad, "Speed control of five-phase IPMSM through PI, SMC and FITSMC approaches under normal and open phase faulty conditions," *Automatika Journal for Control, Measurement, Electronics, Computing and Communications*, vol. 58, no. 4, pp. 506-519, doi: 10.1080/00051144.2018.1478928.

[26] K. Zhou, M. Ai, Y. Sun, X. Wu and R. Li, "PMSM Vector Control Strategy Based on Active Disturbance Rejection Controller," *Energies*, vol. 12, no. 20, pp. 1-19, doi: 10.3390/en12203827.

[27] H. Benbouhenni, "Seven-level direct torque control of induction motor based on artificial neural networks with regulation speed using fuzzy PI controller," *Iranian Journal of Electrical and Electronic Engineering*, vol. 14, no. 1, pp. 85-94, 2018, doi: 10.22068/IJEEE.14.1.85.

BIOGRAPHIES OF AUTHORS

Abdellah Boucha was born in 1982 at Bechar-Algeria. He received the electronical engineering diploma option: Control from the university of Bechar, Algeria in 2006, and the magister degree option: Automatic from the University of USTO Oran, Algeria in 2015. He is aPhD student in the Electrical Engineering at the University of Bechar since 2016. His research interests include electric drives control, electronic, command and automatic. He can be contacted at email: boucha_a@yahoo.fr.

Hazzab Abdeldjebar received the state engineer degree in electrical engineering in 1995 from the University of Sciences and Technology of Oran (USTO), Algeria the M.Sc. degree from the Electrical Engineering Institute of the USTO in 1999, and the Ph.D. degree from the Electrical Engineering Institute of the USTO in 2006. He is currently professor of electrical engineering at University of Bechar, Bechar, Algeria, where he is Director of the Research Laboratory of Control Analysis and Optimization of the Electro-Energetic Systems. His research interests include power electronics, electric drives control, and artificial intelligence and their applications. He can be contacted at email: a_hazzab@yahoo.fr.

Khessam Medjdoub was born in 1984 at Naama-Algeria he's received the electrical engineering diploma from Bechar University, Algeria in 2009, and the Master degree from the University Sidi bel abbes Algeria in 2011 and the Ph.D. degree from the Electrical Engineering University of Bechar, Bechar, Algeria in 2017. He is currently professor of electrical engineering at Institute of science and technology, University center Salhi Ahmed Naama, Algeria. His research interests include power electronics, electric drives control, and artificial intelligence and their applications. He can be contacted at email: Khessam@cuniv-naama.dz or Khessam.medjdoub@hotmail.fr.